DET. DELLE ANISOTROPIE DI VELOCITÀ DELLE ORBITE DELLE GALS IN AMMASSO

Integral VDP velocity dispersion profile

Analytical models for cl. TEORIA

based on the JEANS Eq. (e.g. Merritt 87)

same Φ potential
same T kinetic energy

$\sigma_{obs}(r_i)$ profile

anisotropy parameter

isotropic case
$\beta = 0$

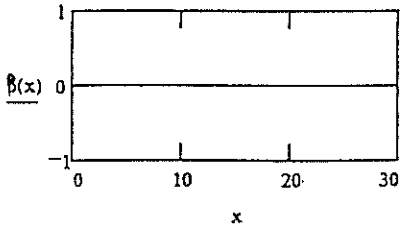

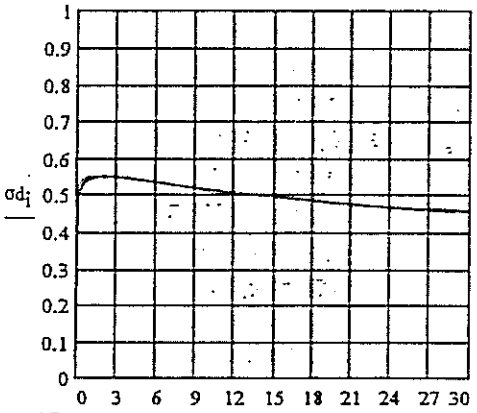

$$\beta(r) = \frac{r^2}{r^2 + r_0^2}$$ velocity anisotropy

$r_i = \frac{r}{r_c}$ r_i (projected distance)

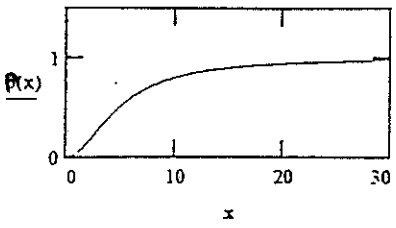

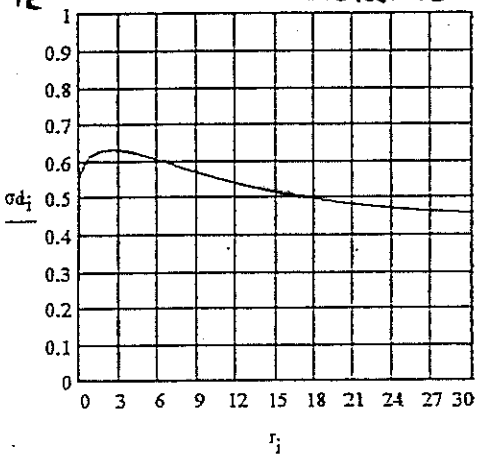

external radial orbits
$\beta > 0$

$\beta = 1$ completely radial

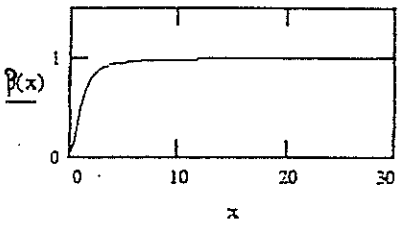

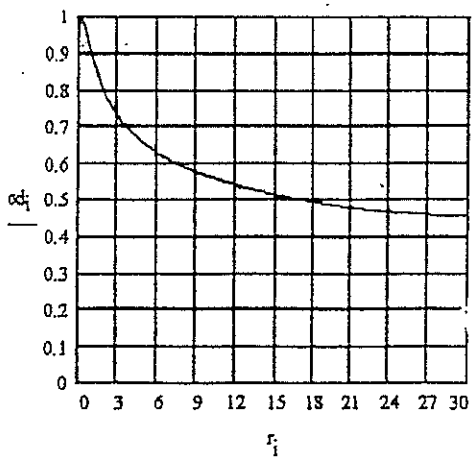

To avoid possible velocity anisotropies we have to adopt the global σ_{los} !

related to the total gravitational potential

Integral Velocity Dispersion Profiles and Velocity Anisotropies

DATI

(MG et al. 1996, Fadda et al. 1996, MG et al. 1998)

Analysis of integral velocity dispersion profile of nearby clusters.
Velocity anisotropies+ DM distribution⇒trend of profiles

Possible anisotropies do not affect global estimate: a flat profile in external region ⇒no longer effect of anisotropies.

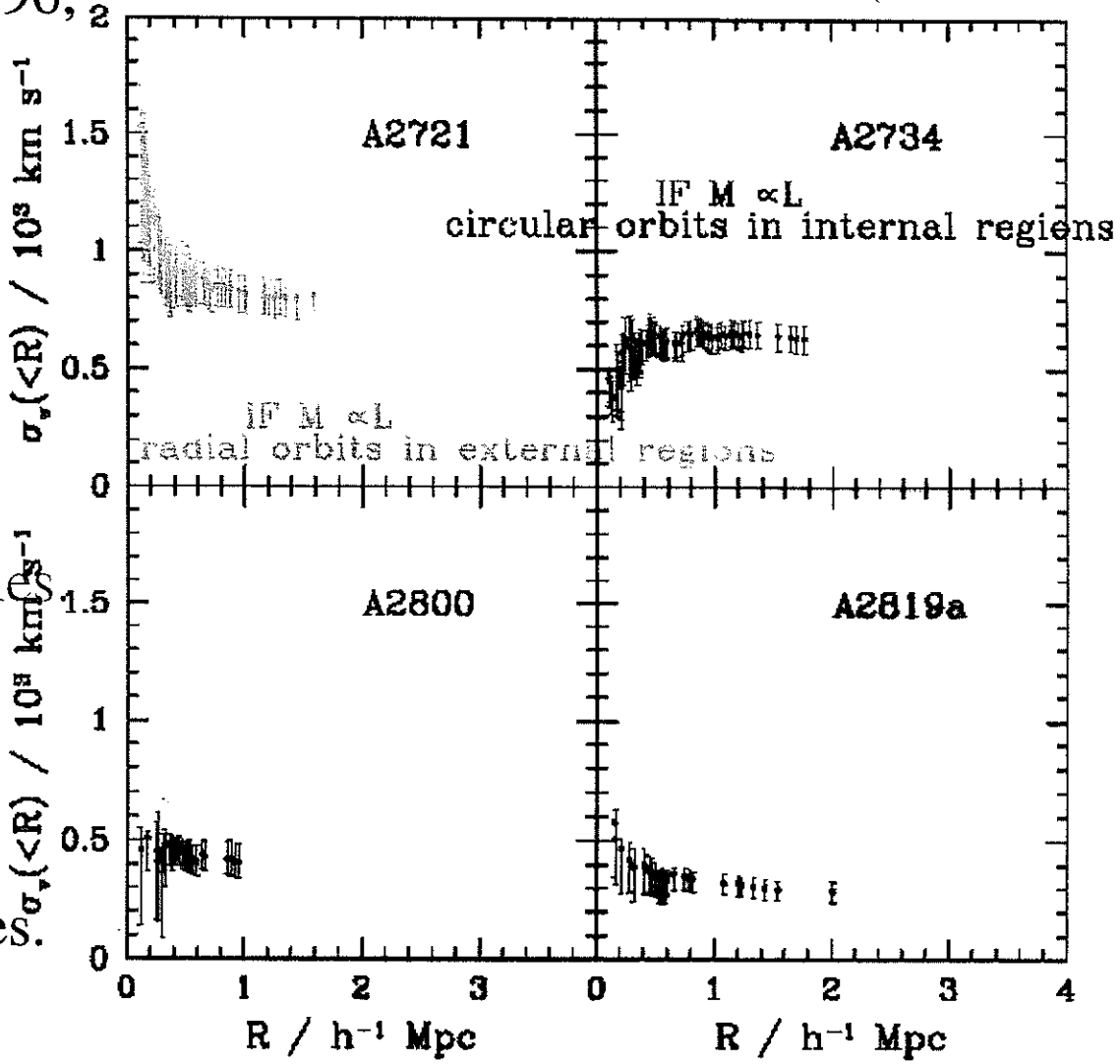

Velocity Dispersion Profiles

DISTANT CLUSTERS

The behaviour of σ_v profiles
is consistent with that of nearby clusters

BUT... some clusters suffer for the poor sampling
and/or small spatial extension

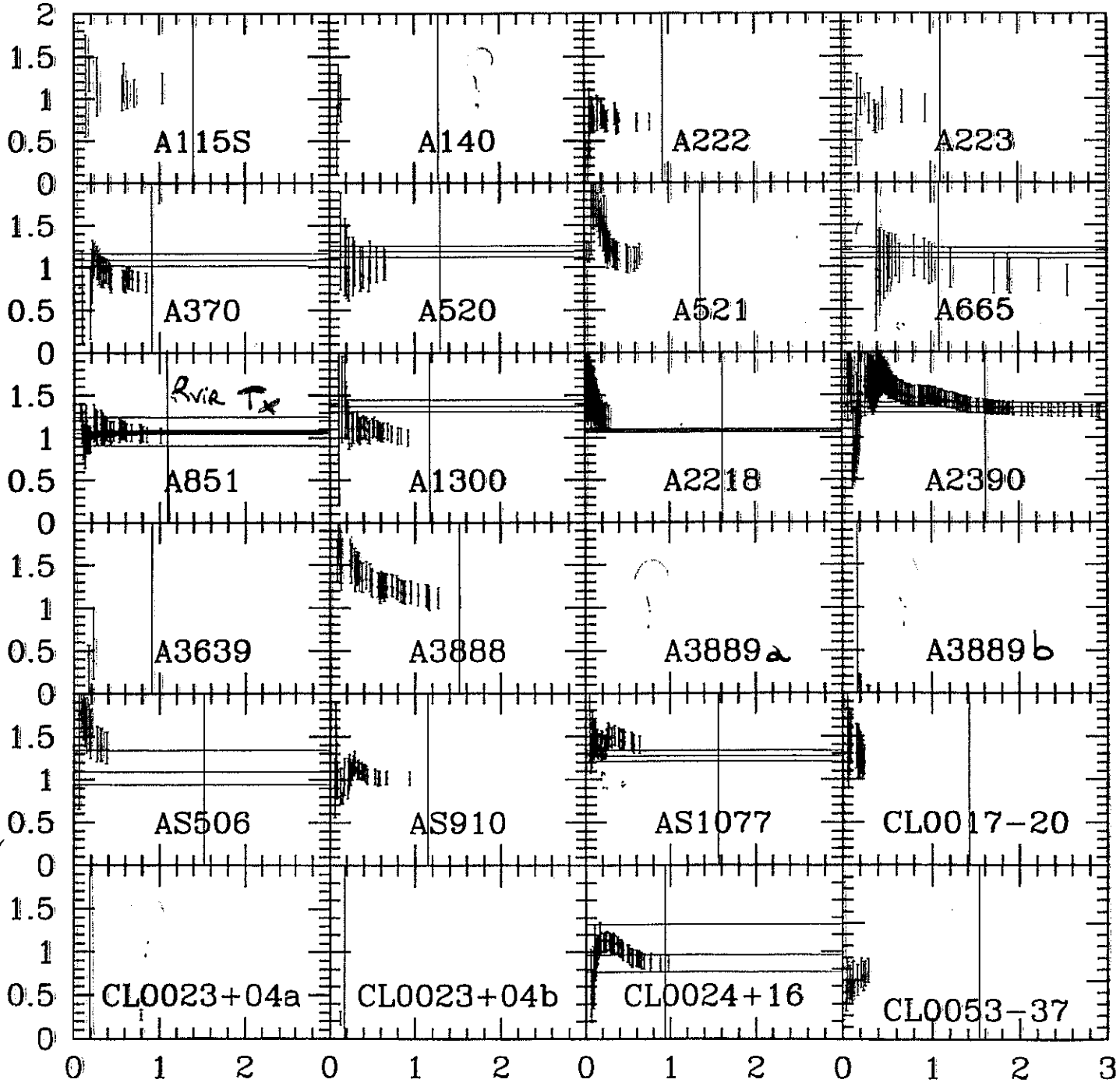

profili di dispersione "integrati" di velocità

OSSERVAZIONI

Velocity Dispersion Profiles and Velocity Anisotropies

(with Giuricin, Mardirossian, Mezzetti, and Boschin 1998, ApJ 505, 74)

Ensemble cluster built with gals of 160 nearby clusters⇒observational profile

Jeans eq.+ mass distribution+assumption for v–anisotropy⇒theoretical profile.

Mass–follows–light assumption

Velocity anisotropy parameter $\beta(\mathbf{r})=1-\sigma_\tau^2(\mathbf{r})/\sigma_r^2(\mathbf{r})=0$:

χ^2 goodness of fit is 96%.

The "average" cluster has isotropic velocities!

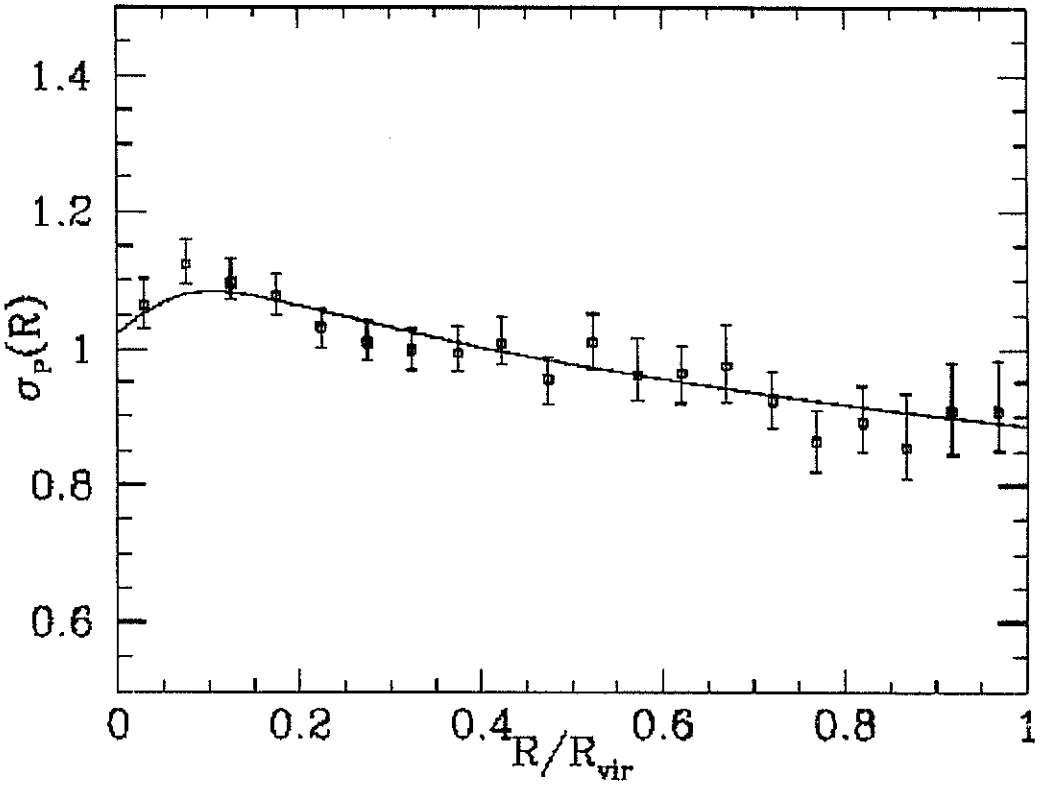

⇒Mean surface term correction to virial mass about 20%.

Profili di dispersione di velocità differenziali TEORIA CFR. DATI

Velocity Dispersion Profiles and Velocity Anisotropies

(coll. with Giuricin, Mardirossian, Mezzetti, and Boschin 1998, ApJ 505, 74)

3 families of clusters (for $\neq \sigma_v$ in central regions/σ_{TOT})⇒3 ensemble clusters.

Jeans eq.+ mass distribution+assumption for anisotropy⇒theoretical profile

$M \propto L$

$$\beta(r) = 1 - \sigma_\tau^2(r)/\sigma_r^2(r)$$

Radial orbits in external regions (infall of galaxies?);
isotropic orbits (violent relaxation?);
circular orbits in internal regions (secondary relaxation phenomena?).

⇒Surface term correction to virial mass about 20–40%.

Clusters may be characterized by different anisotropies...
different stages of evolution?

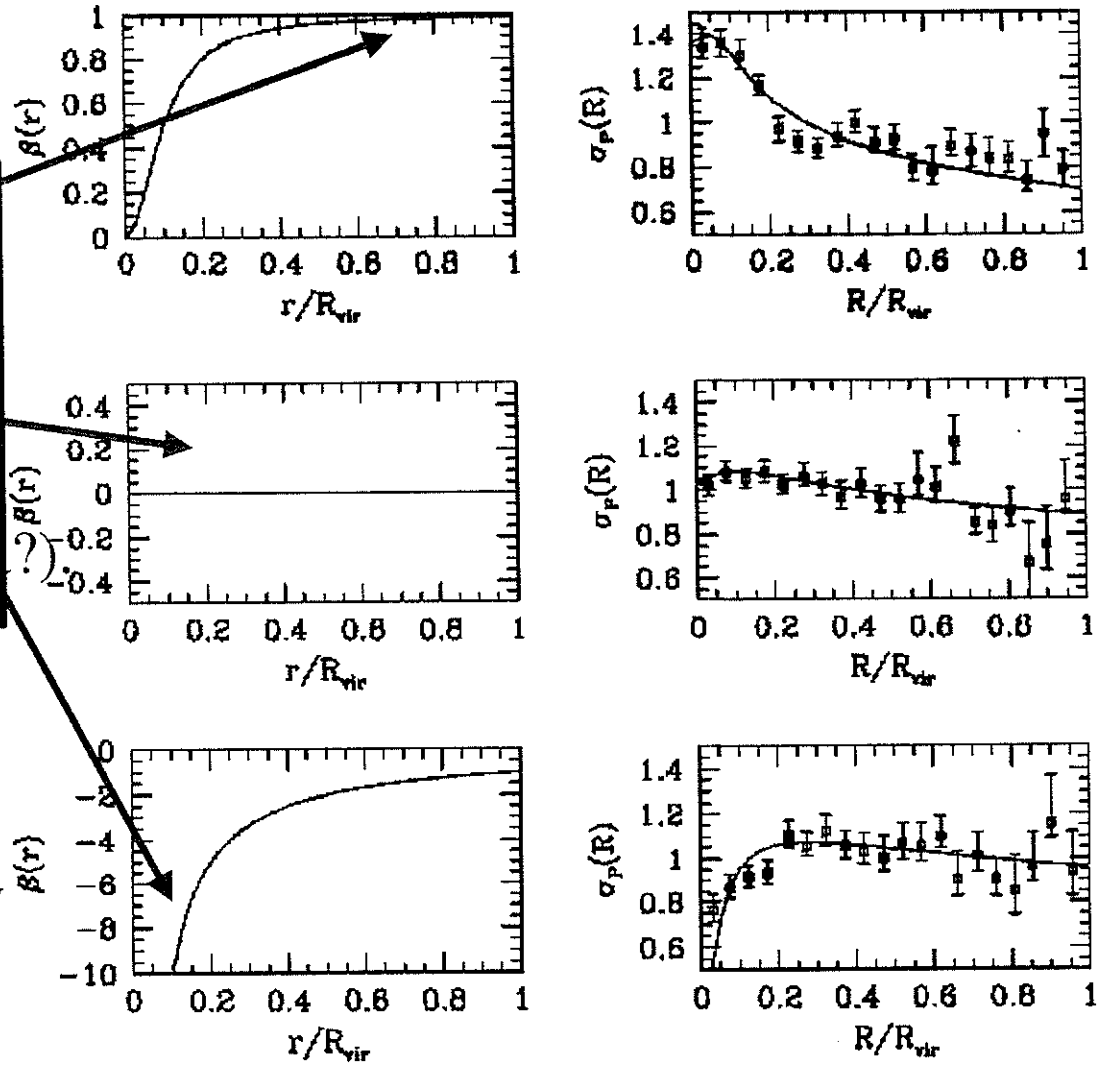

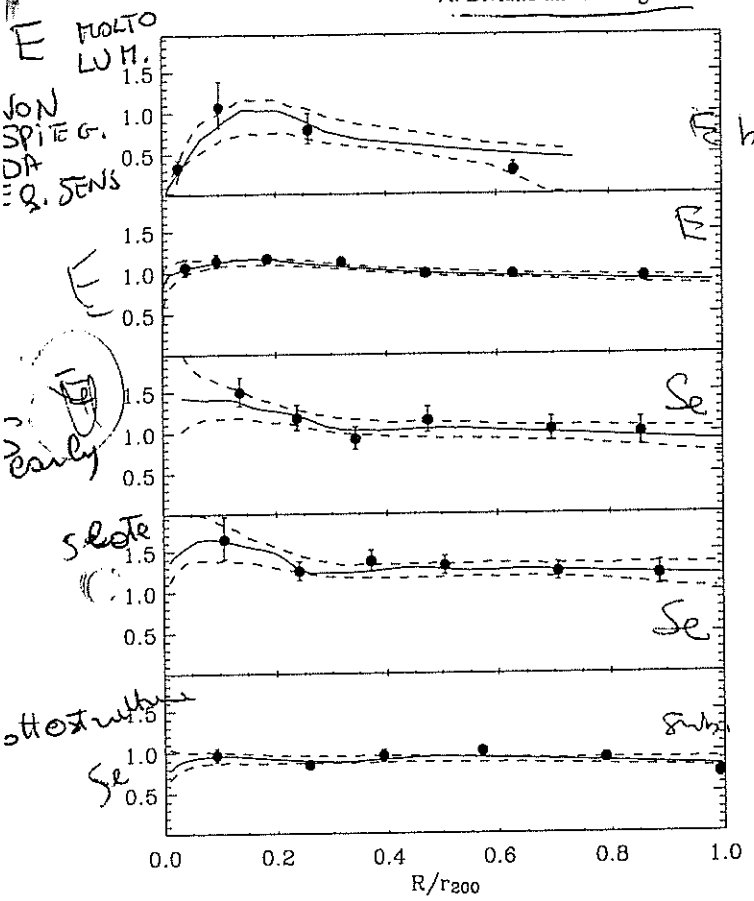

Fig. 2. The best LOWESS estimate (heavy line) of $\sigma_p(R)$, together with the 68% confidence levels (dashed lines), for each of the 5 galaxy classes, *from top to bottom*: E_{br}, Early, S_e, S_l, Subs. The filled circles with error bars indicate binned biweight estimates of $\sigma_p(R)$. The scale on the y-axis is in units of the global cluster velocity dispersion, calculated for all galaxies irrespective of type.

To our knowledge, this is the first time that the number-density and velocity-dispersion profiles for these 5 cluster galaxy classes have been derived with such accuracy and in such detail. Therefore, we briefly comment on the qualitative nature of the different $I(R)$, $\nu(r)$ and $\sigma_p(R)$ before proceeding with the analysis.

Among galaxies outside substructure, the E_{br} have the steepest density profile in the centre, followed by the Early, the S_e, and the S_l. This is a clear manifestation of the morphology-density relation (e.g. Dressler 1980), and of luminosity segregation (e.g. Rood & Turnrose 1968 and Paper XI). Interestingly, the density profiles of both S_e and S_l decrease towards the cluster centre, a clear indication that these galaxies avoid the central cluster regions. On the contrary, E_{br} are mostly found in the central cluster regions.

The Subs galaxies have a number-density profile that is rather steep in the centre, but shows a weak "plateau" at $\sim 0.6\, r_{200}$. Note that the number density profile of this galaxy class could, in principle, be biased by systematic effects due to the selection procedure of the members of substructures, which might result in a radius-dependent detection efficiency. A comparison of the de-projected number densities of the Subs-class galaxies and of the bulk of the galaxies outside substructures, viz. the Early-class galaxies (right-hand panels of Fig. 1), shows that, within $\sim 0.6\, r_{200}$, the two profiles have essentially identical logarithmic slopes. Beyond $\sim 0.6\, r_{200}$ the number-density profile of the Subs galaxies is quite a bit flatter than that of the Early galaxies, until it steepens again beyond $\sim 1.0\, r_{200}$. This was already noted in Paper XI. A comparison of the number-density profile of the Subs galaxies with that obtained by De Lucia et al. (2004) from their numerical models of substructures in cold dark matter haloes gives a similar result. The logarithmic slope between $0.1\, r_{200}$ and $0.8\, r_{200}$ of the number-density of haloes with masses $\sim 10^{13}\, M_\odot$ is about -1.6, not very different from that of the Subs galaxies which is -1.5.

The velocity dispersion of the E_{br} strongly decreases towards the centre, with a slower but equally large decrease outwards (remember that *all* velocity dispersions are normalized by the same, global velocity dispersion calculated for *all* galaxies irrespective of type). The special formation history and location of the E_{br} at the bottom of the cluster potential well is reflected in their very low central velocity dispersion. In contrast, galaxies of the Early class have a rather flat velocity-dispersion profile, changing by only $\approx \pm 20\%$ over the virial region. The velocity-dispersion profiles of S_e and S_l are rather similar, starting at high values near the centre with a fairly rapid decrease out to $r \approx 0.3\, r_{200}$, and flattening towards larger projected distances. Yet, the velocity dispersion of the S_l is larger than that of the S_e (and, in fact, of any other class) at all radii. It is perhaps interesting to note that the velocity-dispersion profiles of S_e and S_l are remarkably similar to those of, respectively, the "backsplash" and infalling populations of subhaloes found in the numerical simulations of Gill et al. (2004).

Finally, the velocity-dispersion profile of the Subs class is very "cold" and flat, even flatter and "colder" than that of the Early class. One might wonder if this is due to the procedure by which the galaxies of the Subs class were selected, but it is very unlikely that the velocity dispersion of the Subs class is biased low by the selection. If anything, the actual velocity dispersion of the subclusters is overestimated because the internal velocity dispersion of the subclusters has not been corrected for. In Sect. 6.4 we discuss several estimates for the real velocity-dispersion profile, i.e. corrected for internal velocity dispersion and possible bias due to the selection.

4. The mass profile

In addition to the observed $I(R)$-, $\nu(r)$- and $\sigma_p(R)$-profiles presented in Sect. 3 we also need an estimate of the mass profile $M(<r)$ for a determination of the $\beta(r)$-profiles. The mass profile that we will use here is the one that was derived in Paper XII, from the number density and velocity-dispersion profiles of the Early-class galaxies. As discussed in detail in Paper XII, the Early-class galaxies are likely to be in equilibrium with the cluster potential, as the formation of most of them probably antedates their entry into the cluster, so that they have had ample time to settle in the potential. In Paper XII we also showed that galaxies of the Early class have a nearly isotropic velocity distribution; this follows from an analysis of the shape of the distribution of their line-of-sight velocities. More specifically, assuming a constant velocity anisotropy for the

N(v) ⇒ ORBITE
MOMENTI SUCCESSIVI ALL'EQ. DI JEANS

distribution as a function of projected radius. In effect, this technique would require any model of Coma to be consistent not only with the Jeans equation, but also with the more detailed Boltzmann equation from which the Jeans equation is derived. No one has yet described the best way to carry out this task (nor is there any cluster that is both sufficiently well observed, and convincingly close to equilibrium, to justify such an analysis). In the case of Coma, one way to make use of the extra information contained within the full velocity distribution function is illustrated in Figure 2. The overall velocity histogram appears marginally most consistent with a high–mass, radial–orbit model; a model with low mass and circular orbits appears strongly inconsistent. There are, however, a number of reasons to be cautious about this comparison. The shape of the velocity histogram can be strongly affected by processes such

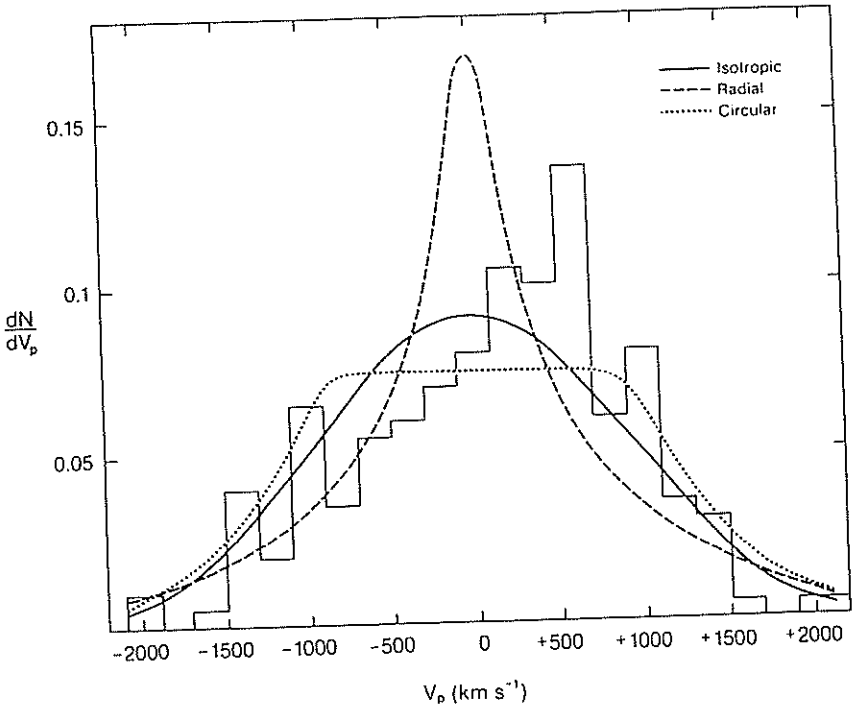

Fig. 2 Velocity histogram for galaxies in Coma. The three curves are derived from models in which the galaxy orbits are isotropic, radial, and circular; the dark matter distributions have been adjusted to give the same line–of–sight velocity dispersion profile in each case. (From Merritt, *Ap. J.*, **313**, 121.)

as rotation and infall which we have so far neglected. In fact, inspection of Figure 2 reveals a possibly significant ($\sim 97\%$ confidence) degree of skewness in the observed distribution. Cluster rotation by itself would tend to broaden

not exhibit significant rotation (Rood et al. 1972). However there is good reason to believe that contamination by foreground galaxies might explain the low–velocity "tail". De Lapparent, Geller and Huchra (1986) show that the Coma cluster appears to sit at the intersection of a number of large–scale galaxy "shells", one of which lies nearly along the line of sight to Coma. These foreground galaxies could significantly affect the form of the overall velocity histogram, even if they have little effect on the inferred dynamics of the central regions.

A number of other techniques have been discussed for constraining the orbital kinematics of galaxies in clusters. Pryor and Geller (1984) attempted to use the observed tidal radii and gas content of galaxies in Coma to put limits on their orbital pericenters, and hence on the degree of velocity anisotropy. Their result (that the Coma cluster is close to isotropic within $1h^{-1}$ Mpc) is strongly dependent on the uncertain physics of tidal truncation and gas dynamical ablation; furthermore those authors only considered models in which the dark matter is distributed like the galaxies, while in fact the available velocity data imply a fairly tight relation between the mass distribution and the galaxy orbits, as discussed above. O'Dea, Sarazin and Owen (1987) used the orientation of "narrow angle tail" radio sources in clusters to constrain the distribution of galaxy orbits, under the assumption that the radio–luminous plasma ejected by a moving galaxy is bent into a tail which marks the path taken by the galaxy through the cluster. Since most clusters contain only a few such radio sources (Coma, for instance, contains only one), those authors were forced to superpose data from many clusters. They obtained the surprising result that galaxy orbits in the inner $\sim 0.5h^{-1}$ Mpc of their clusters are strongly *radial*; at large radii the distribution of tail orientations appears to be random. The correct interpretation of this result will probably have to await a better understanding of the gas ablation process. It may be, for instance, that the probability of observing a galaxy as a narrow angle tail depends strongly on its velocity with respect to the intracluster gas, in which case the observed sample could be kinematically biased.

For a long time it was hoped that X–ray observations of hot intracluster gas would resolve the indeterminacy of cluster masses. The equation of hydrostatic equilibrium, in spherical symmetry, states

$$\frac{d\Phi}{dr} = \frac{GM(r)}{r^2} = -\frac{1}{\rho_g}\frac{dP_g}{dr} = -\frac{1}{\rho_g}\frac{d}{dr}\left(\rho_g k T_g\right), \qquad (10)$$

where ρ_g and T_g are the gas density and temperature. Equation (10) is simpler than the Jeans equation (3) since gas is a collisional fluid with an isotropic pressure; thus the two functions $\{\sigma_r(r), \sigma_t(r)\}$ are replaced by one, $T_g(r)$. Furthermore, the statistical accuracy of a mass determination based on the X–ray emitting gas can always be increased by lengthening the integration time, whereas the number of bright galaxies in a cluster is limited. Unfortunately, the spatial resolution of the spectral instruments on past X–ray satellites has not been very good, and at present there is no cluster (with the possible exception of Virgo) for which we have an accurate determination of $T_g(r)$. This problem is capable of solution; future satellites, such as AXAF, should yield accurate temperature profiles and hence accurate masses for nearby clusters. However